Association Constants and Reaction Dynamics of Metal Ions Bound to Anionic Micelles

Henry Ziemiecki and W. R. Cherry*

Contribution from the Department of Chemistry, West Virginia University, Morgantown, West Virginia 26506. *Received December 1, 1980*

Abstract: The association constants (K) of seven metal ions (Cs^+, Tl^+, Cu^{2+}, Co^{2+}, Mn^{2+}, Cr^{3+}, and Eu^{3+}) to sodium dodecylsulfate (SDS) micelles have been determined. There does not appear to be any relationship between the metal ion's charge and its association constant. In general, these deviations from the Bjerrum theory of ionic association can be rationalized by considering the chemistry of the specific ion. The rate constants for quenching of pyrene fluorescence by the ions in both homogeneous and micellar phases are also reported. From the comparison of these rate constants, it is concluded that the "water channel" model proposed previously is not operative. Instead, the results indicate that the quenching mechanism in the micelle is similar to the mechanism in homogeneous solution.

In the past several years, micelles have been extensively studied as membrane models, in energy storage systems, and as catalysts for organic reactions.[1] Micelles are the simplest example of a multiphase system and as such have been used to generate substantial charge separation.[2] Furthermore, micellar solubilization can not only result in catalysis but also alter the course of a reaction.[3]

In order for a micelles to be effective in a particular role, the substrate(s) must be somehow associated with the micelle. This may occur by solubilization of the substrate into the micelle's hydrophobic region. Alternatively, a species may be distributed in both the bulk or aqueous phase and on the micelle's surface. In this case, an equilibrium constant can be defined as shown below, where M refers to a micelle, S to a substrate, and a to the aqueous phase.

$$\mathrm{M} + \mathrm{Sa} \rightleftharpoons \mathrm{M}\cdots\mathrm{S} \qquad S = \frac{[\mathrm{M}\cdots\mathrm{S}]}{[\mathrm{M}][\mathrm{Sa}]} \tag{1}$$

These phenomena of solubilization and association have been examined by using X-ray diffraction, absorption and NMR spectroscopy, and ESR spin labeling techniques.[4] Recently, another method, involving the quenching of luminescent probe molecules, has been developed and has provided information concerning the dynamics of solubilization and association.[5-10]

In order to understand the dynamic events associated with micelle association and the interaction of two species mediated by a micelle, we have systematically examined the association of various metal ions with sodium dodecylsulfate (SDS) micelles as well as the fluorescence quenching rate constants in homogeneous and micellar solution. Several interesting features of the cation/micelle interaction have been uncovered. For example, the apparent charge on a metal ion does not always dictate the magnitude of the binding constant of the metal ion to an anionic micelle. Also, the quenching process does not involve entry of the metal ion into "water channels" of the micelle but rather the association of probe and quencher "through" the micelle wall.

Experimental Section

Sodium dodecylsulfate was washed several times with ether and dried in a vacuum desiccator over $CaCl_2$. Distilled water was again distilled from $KMnO_4$ in a glass apparatus. Pyrene was sublimed once and recrystallized twice and anthracene was codistilled with ethylene glycol. The metal salts (either the sulfate or chloride) were used as received.

In a typical quenching run, the probe (5×10^{-5} M) was solubilized in a solution of 0.025 M SDS. After being stirred overnight, this solution was filtered and divided into several fractions. Solid SDS was added to each fraction to adjust the final surfactant concentration to the desired level.

The homogeneous quenching rate constants were determined in an 8:2 mixture of water and ethanol. The Stern-Volmer plots were all linear and the fluorescence lifetime of pyrene in the absence of quencher was determined to be 304 ns.

The fluorescence intensities were measured on an Amico Bowman spectrophotofluorometer. The micelle samples were not degassed as oxygen did not appear to influence the final results.

The fluorescence lifetimes were measured by the time-correlated single-photon counting method.[11] In this case, the homogeneous as well as surfactant solutions were degassed by Ar bubbling.

Results

1. Quenching in Micellar Solutions. The Stern-Volmer plots for the quenching of pyrene (P^{*1}) by Eu^{3+} at several concentrations of surfactant are shown in Figure 1. They are all nonlinear in the lower concentration range but become linear at high concentrations of Eu^{3+}. This behavior has been noted previously and has been attributed to static and dynamic quenching. Atik and Singer[5] have derived an expression for the entire quenching plot.

$$I_0/I = (1 + \beta k_q^{\mathrm{m}} K \tau_f [\mathrm{Q_T}])/(1 + \alpha\beta k_q^{\mathrm{m}} K \tau_f [\mathrm{Q_T}]) \tag{2}$$

In this equation, I_0 and I are the fluorescence intensities in the absence and presence of quencher, Q, at a total concentration of $[Q_T]$, k_q^m is the bimolecular quenching rate constant of the probe by Q, τ_f is the fluorescence lifetime of the probe, K is the binding constant of Q, α is the fraction of micelles withoug a quencher, and $\beta = (1 - K[M])^{-1}$ where [M] is the micelle (not surfactant) concentration. The micelle concentration was determined in the usual manner, using 8.1×10^{-3} M/l and 62 as the CMC and aggregation number of SDS, respectively.[1a]

As the total concentration of Q increases, the value of α approaches 0. Hence, at high values of Q, eq 2 reduces to the usual form of a Stern-Volmer equation but with a different slope (eq 3). The linear region of the quenching plot can then be used to

$$I_0/I = 1 + \beta k_q^{\mathrm{m}} K \tau_f [\mathrm{Q_T}] \tag{3}$$

obtain a value for K by simply evaluating the slopes in the linear

* Address correspondence to this author at the Department of Chemistry, Louisiana State University, Baton Rouge, Louisiana 70803.

(1) (a) Fendler, J. A.; Fendler, E. J. "Catalysis in Micellar and Macromolecular Systems"; Academic Press: New York, 1975; (b) Mittal, K. I. "Micellization, Solubilization, and Microemulsions"; Plenum Press, New York, 1977; Vol. 1 and 2.

(2) Mario Y.; Braun, A. M.; Gratzel, M. *J. Am. Chem. Soc.* **1979**, *101*, 567, 579.

(3) Cherry, W. R.; Turro, N. J. *J. Am. Chem. Soc.* **1978**, *100*, 7431.

(4) (a) Lindman, B.; Lindblom, G.; Wennerström, H.; Gustavsson, H. in ref 1b, Vol. 1, p 195. (b) Hasegawa, A.; Michihara, Y.; Miura, M. *Bull. Chem. Soc. Jpn.* **1970**, *43*, 3116. Oakes, J. *J. Chem. Soc., Faraday Trans. 2* **1973**, *69*, 1321. (c) Reference 1a, pp 43-83.

(5) Atik, S. S.; Singer L. A. *Chem. Phys. Lett.* **1978**, *59*, 519.

(6) Infelta, P. P.; Gratzel, M.; Thomas, J. K. *J. Phys. Chem.* **1974**, *78*, 190. Almgrem, A.; Grieser, F.; Thomas, J. K. *J. Am. Chem. Soc.* **1979**, *101*, 2021.

(7) Yekta, A.; Aikawa, M.; Turro, N. J. *Chem. Phys. Lett.* **1979**, *63*, 543. Yekta, A.; Turro, N. J. *J. Am. Chem. Soc.* **1978**, *100*, 5951.

(8) Ziemiecki, H.; Holland, R.; Cherry, W. R. *Chem. Phys. Lett.* **1980**, *73*, 145.

(9) Dederen, J. C.; van der Auweraer, M.; de Schryver, F. C. *Chem. Phys. Lett.* **1979**, *68*, 451.

(10) Escubi-Perez, J. R.; Nome, F.; Fendler, J. H. *J. Am. Chem. Soc.* **1979**, *99*, 7749.

(11) Ware, W. R. In "Creation and Detection of the Excited State", Lamola, A. A., Ed.; Marcel Dekker: New York, 1971; p 213.

0002-7863/81/1503-4479$01.25/0

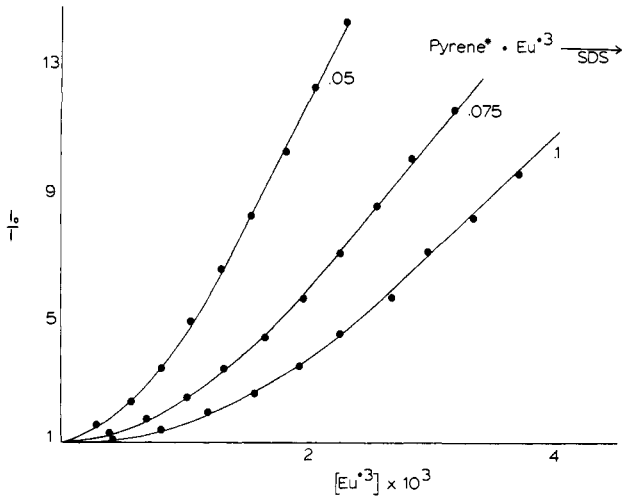

Figure 1. The Stern–Volmer plots for the quenching of pyrene fluorescence by Eu^{3+} at 0.05, 0.075, and 0.1 M concentrations of SDS.

Table I. Binding Constants of Various Metal Ions to SDS Micelles

metal ion	probe[a]	K
Cs^+	P	4900 ± 2000[b]
Tl^+	P	47200 ± 10000
Cu^{2+}	A	8800 ± 2400[c]
	P	11000 ± 2000[b]
		10000 ± 1000[d]
		1400[e]
Co^{2+}	P	36600 ± 3000
Mn^{2+}	P	126000 ± 30000
Eu^{3+}	P	130000 ± 20000
Cr^{3+}	P	3700 ± 1000

[a] P = pyrene, A = anthracene. [b] From lifetime quenching, see text. [c] Reference 8. [d] Reference 9. [e] Grätzel, M.; Thomas, J. K. *J. Phys. Chem.* 1974, *78*, 2248.

region as a function of micelle concentration. The slope (S) at a particular [M] is given by

$$S = \beta k_q^m K \tau_f \tag{4}$$

Recalling that $\beta = (1 + K[M])^{-1}$, eq 4 can be rewritten as

$$S = k_q^m K \tau_f / (1 + K[M]) \tag{5}$$

Simple rearrangement of eq 5 leads to

$$1/S = 1/k_q^m K \tau_f + [M]/k_q^m \tau_f \tag{6}$$

which can be used to obtain K. A plot of $1/S$ vs. [M] should be linear with a slope of $1/k_q^m \tau_f$. Hence, K can be obtained by dividing the slope by the intercept. Such a plot for the quenching of pyrene fluorescence by Eu^{3+} is shown in Figure 2. As expected, the plot is linear and a value of the association constant of Eu^{3+} to SDS micelles is evaluated to be 130000 (±20000) M^{-1}. Results for the other metal ions are shown in Table I.

The slope in Figure 2 is $(k_q^m \tau_f)^{-1}$ where k_q^m is the rate constant for the quenching of pyrene fluorescence by a metal ion that has already been bound to the micelle. The values for k_q^m were determined by using the slopes of metal quenching plots and the lifetime of pyrene in micellar solution (=296 nm). These values are shown in Table II.

An alternative approach for determining K and k_q^m involves the analysis of the nonlinear decay of the pyrene fluorescence in the presence of quenchers. The general equation describing fluorescence decay is given by (7),[9] where Q is a quencher

$$\ln i(t) = \ln i(0) - \left(k_f + \frac{(k_+[Q_a] + k_e[Q_m])k_q^m}{k_- + k_e[M] + k_q^m} \right) t - \frac{(k_+[Q_a] + k_e[Q_m])k_q^{m2}}{(k_- + k_e[M])(k_- + k_e[M] + k_q^m)^2} \{1 - \exp[-(k_q^m + k_e[M] + k_-)t]\} \tag{7}$$

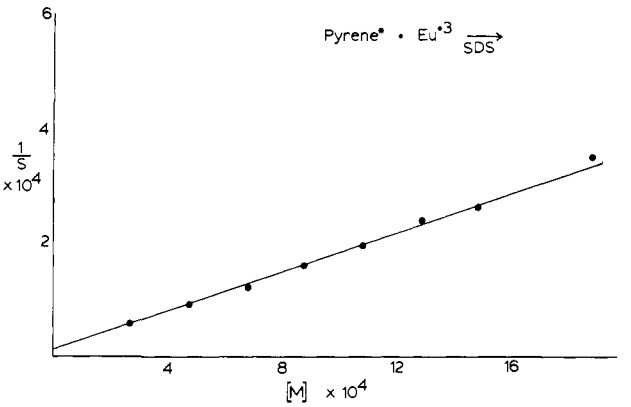

Figure 2. The plot of S^{-1} vs. micelle concentration for Eu^{3+}.

Table II. Rate Constants for the Quenching of Pyrene Fluorescence by Metal Ions in Both Micellar and Homogeneous Phases

metal ion	k_q^m	$k_q^{H_2O}$	RP[a]
Cs^+		2.2×10^7	−2.923
Tl^+	1.4×10^7	3.2×10^9	−0.34
Cu^+	2.8×10^7 [b]	5.3×10^9 [b]	0.158
Co^+	3.9×10^6	3.9×10^8	
Mn^+	2.6×10^6	2.0×10^8	
Eu^+	1.8×10^7	7.1×10^8	−0.43
Cr^+	1.4×10^7	1.9×10^9	−0.41

[a] RP = reduction potential. Relative to the Standard Hydrogen Electrode, "CRC Handbook", Chemical Rubber Co.: Cleveland, OH, 1969; 50th ed.. [b] Taken from ref 9 for the quenching of methylpyrene by Cu^{2+}. The homogeneous phase was H_2O.

(subscript a = aqueous, m = micelle, t = total), k_f is the reciprocal of pyrene's fluorescence lifetime in the absence of quenchers, k_+ and k_- are the entrance and exit rate constants of Q onto or off of the micelle ($K = k_+/k_-$), and k_e is the rate of exchange of a quencher between micelles. When $k_q^m >> k_e[M] + k_-$, eq 7 reduces to

$$\ln i(t) = \ln i(0) - \left(k_f + \frac{(k_+ + k_e K[M])}{(1 + K[M])}[Q_T] \right) t - \frac{K[Q_T]}{(1 + K[M])}(1 - \exp[-k_q^m t]) \tag{8}$$

where the following identities (eq 9 and 10) were used in the derivation. The values of k_+, k_-, k_e, and k_q^m can be determined

$$K = k_+/k_- = [Q_m]/[M][Q_a] \tag{9}$$

$$[Q_T] = [Q_a] + [Q_m] \tag{10}$$

by analysis of the nonlinear decay of pyrene at different quencher and micelle concentrations. While more tedious, this method does provide more information than the simple quenching experiment. Such an analysis has been done for Cu^{2+} and Cr^{3+} and the results agree with those obtained from the static quenching method (Table I).

In the case of Cs^+, k_q^m is small and the fluorescence decay is linear even at high concentrations of Cs^+. The decay is now given by eq 11 and K can be determined by examining the (linear)

$$\ln i(t) = \ln i(0) - \left[k_f + \frac{(k_+[Q_a] + k_e[Q_m])k_q^m}{k_- + k_e[M]} \right] t \tag{11}$$

fluorescence decay as a function of quencher and micelle concentrations. Such decay curves for pyrene in SDS at various concentrations of Cs^+ are shown in Figure 3. As can be seen, the decays are all linear, typical of quenching that follows eq 11.

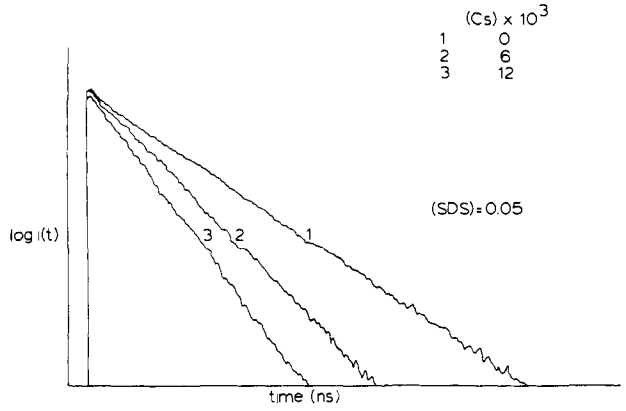

Figure 3. The fluorescence decay of pyrene at various concentrations of Cs^+ in 0.05 M SDS solution.

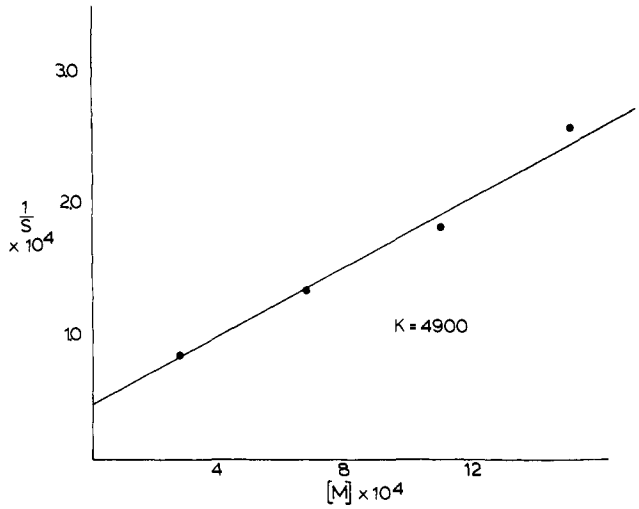

Figure 4. The plot of S^{-1} vs. micelle concentration for Cs^{2+}.

When these decay curves are analyzed in the usual Stern–Volmer method, a straight line results whose slope is given by eq 12.

$$\text{slope} = S = \frac{k_+ k_q^m}{(k_- + k_q^m)(1 + K[M])} \quad (12)$$

$$1/S = \frac{(k_- + k_q)}{k_+ k_q} + \frac{K(k_- + k_q)[M]}{k_+ k_q} \quad (13)$$

Simple rearrangement yields eq 13, which predicts a linear relationship between $1/S$ and the micelle concentration. Such a plot is shown in Figure 4 and is indeed linear. The binding constant is then easily evaluated as 4900 M^{-1}. Unfortunately, k_q cannot be evaluated in this approach since there are two knowns (the slope and intercept) and three unknowns (K, k_q, and k_+ or k_-).

2. Homogeneous Solution. The quenching of pyrene in an 8:2 water:ethanol mixture by all mettal ions exhibits Stern–Volmer kinetics. The rates ($k_q^{H_2O}$) are shown in Table II. These rate constants have been determined by following both the fluorescence intensity and lifetime quenching. Both methods gave equivalent values of $k_q^{H_2O}$.

The expected mechanism of fluorescence quenching involves the transfer of an electron from excited pyrene to the metal ion. Consequently, $k_q^{H_2O}$ should be related to the one-electron reduction potential of the metal ions and, as can be seen from Table II, this trend is generally followed. The most easily reduced ion, Cu^{2+}, is the most efficient quencher and rates decrease as the reduction potential decreases. In the case of Cs^+, the reduction potential is so negative that electron transfer is highly unlikely and the quenching mechanism probably involves heavy-atom-induced intersystem crossing.

Discussion

1. Binding Constants. Previous work on the association of ions has indicated that electrostatics is an important factor. Bjerrum has developed an equation relating the equilibrium constant to an exponential function of Z_i/r_i, where Z_i and r_i are the charge and radius of a metal ion.[12] This has been verified for numerous dilute electrolytes, including the association constants of metal ions to a sulfate ion.[13]

For the binding of metal ions to SDS anionic micelles, the Bjerrum theory has been successful at rationalizing the previously determined trends in association constants. Mukerjee et al.[14] and Robb et al.[15] have shown that, qualitatively, the binding of alkali metal ions to SDS micelles increases as the atomic number increases. At this point, it should be stressed that the hydrated and ionic radii of a metal ion are different. While the radii[16] of Li^+ and Cs^+ are 0.68 and 1.67 Å, their hydrated radii[17] are 3.82 and 3.29 Å. Since Li^+ is larger than Cs^+ in aqueous solution, the Bjerrum theory predicts an increase in the binding constant as the atomic weight increases, which is observed experimentally.

As the charge on a metal ion increases, the association constant is expected to increase. Baumüller et al.[18] have observed this qualitative trend. Conductivity and activity data indicated that the divalent metal ions, Ni^{2+} and Co^{2+}, are bound more strongly to SDS micelles than is Na^+. Similarly, Robb[19] has shown that Gd^{3+} is bound more strongly to SDS than either Mn^{2+} or Cu^{2+}. Finally, Grieser[20] has recently reported qualitative trends in the binding of metal ions to SDS micelles, using pulsed radiolysis. Again, the association appeared to increase as the metal ion's charge increased.

The results reported in Table I indicate that the electrostatic effect cannot be the only factor responsible for the magnitude of the association constant. While one may argue that the expected trend can be observed, there are clearly exceptions, most notably Tl^+ and Cr^{3+}. Furthermore, Mn^{2+} seems to bind more strongly than expected for a divalent ion. However, Mn^{2+} is a d^5 ion and cannot enjoy any crystal field stabilization[16] so that the inner sphere water molecules are amenable to replacement by a sulfate group of the micelle.

In general our results agree with those previously reported. Clearly, the divalent metal ions are bound more strongly than Na^+ (which is bound less strongly than Cs^+). Furthermore, our results are similar to Grieser's for Eu^{3+}, Cu^{2+}, and Mn^{2+}. However, for the thallous ion our value is larger than that reported by Grieser based on both pulsed radiolysis and fluorescence quenching. Interestingly, the lifetime quenching by Tl^+ does not result in nonlinear decay as for Cu^{2+} but rather linear decay much like Cs^+. The analysis used for Cs^+ provides a value of 1200 ± 800 for the association constant of Tl^+ to SDS micelles. However, this is in the low concentration region ($\tau_0/\tau < 3$) and may be simply a tangent to the overall nonlinear quenching plot. Clearly, the large quenching rate constant for Tl^+ (vide infra) indicates a nonlinear behavior should be observed as in the fluorescence intensity quenching plots. Experiments to clarify this anomalous behavior of Tl^+ are currently underway.

In contrast to Tl^+, both the fluorescence intensity and lifetime quenching for Cr^{3+} agree that the metal ion is bound very weakly. The most likely explanation for this small binding constant is that

(12) For an excellent review see Petrucci, S., "Ionic Interactions"; Academic Press, New York, 1971; Vol. 1, p 118.
(13) Izatt, R.; Eatough, D.; Christensen, J. J.; Bartholomew, C. H. *J. Chem. Soc. A* **1969**, 47.
(14) Mukerjee, P.; Mysels, K. J.; Kapauan, P. *J. Phys. Chem.* **1967**, *71*, 4166.
(15) Robb, I. D.; Smith, R. *J. Chem. Soc., Faraday Trans. 1* **1974**, *70*, 287.
(16) Cotton, F. A.; Wilkinson, G. "Advanced Inorganic Chemistry"; Interscience Publishers: New York, 1967.
(17) Nightingale, E. R. *J. Phys. Chem.* **1959**, *62*, 1381.
(18) Baumüller, W.; Hoffman, H.; Ulbright, W.; Tondre, C.; Zana, R. *J. Colloid Interface Sci.* **1974**, *64*, 418.
(19) Robb, I. D., *J. Colloid Interface Sci.* **1971**, *37*, 521.
(20) Grieser, F.; Tausch-Treml, R. *J. Am. Chem. Soc.* **1980**, *102*, 7258.

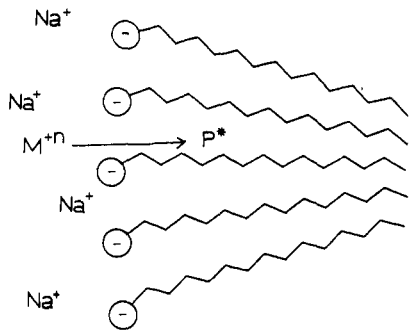

Figure 5. In the water channel model, the metal ion must penetrate the micelle in order for quenching to occur.

$Cr(H_2O)_6^{3+}$ ions can form complex ions in neutral or basic solution.[21] These complex ions can involve the counterion, so the binding constants for $Cr(NO_3)_3$, $CrCl_6$, and $Cr_2(SO_4)_3$ were determined and found to all be within experimental error. Judging from stability constants,[22] the most likely ions present in the micellar solution are $[Cr(H_2O)_5(OH)]^{2+}$ and $[Cr(H_2O)_4(OH)_2]^{+}$. Obviously, these two species will be bound more weakly than $Cr(H_2O)_6^{3+}$. Furthermore, dimeric species can form but usually require boiling of the chromic salt solution.[21] Consequently, it is unlikely that this dimer will form during the course of a quenching experiment. Similar reasoning leads to the conclusion that $Cu(H_2O)_6^{2+}$ can also be partially deprotonated[22] which could explain its low binding constant.

2. Quenching Rate Constants. The rates of quenching in homogeneous and micellar phases are collected in Table II. The k_q^m values for micellar quenching are the rate constants for ions that have already been bound to the micelle. Hence, the relationship of this rate constant to the corresponding rate constant in homogeneous solution will provide information on the mechanism of quenching at the micelle's surface.

There are two likely mechanisms of quenching at a micelle's surface. The first involves the migration of the metal ion into the "water channels" separating the surfactant monomers.[23,24] Once the micelle has been penetrated, the metal ion would be in the vicinity of the excited pyrene molecule and quenching could occur. The second mechanism involves association of the metal ion on the micelle's surface with no penetration of the micelle. It is well known that aromatic compounds are solubilized at the micelle's surface[25] so that quenching can occur by diffusion of the metal ion along the micelle's surface.

The first mechanism is dependent upon the penetration of the metal ion into the micelle as depicted in Figure 5. Clearly, if the metal ion must move any significant distance down the water channel, then there should be a relationship between the ion's size and the effect of a micelle on the quenching rate. The relative quenching rates in micellar and homogeneous phases, as well as both the ionic and hydrated radii of the metal ions, are shown in Table III. There does not seem to be any relationship between the effect of a micelle on the quenching rate and the metal ion's size.

Conversely, the second mechanism suggests a similarity between homogeneous and micellar quenching rate constants. The general kinetic equations for quenching in both phases are shown in Scheme I.[26] An encounter complex is formed at a diffusion-controlled rate, k_d, and results in quenching. The observed k_q will be given by eq 14 and, since $k_{-d} > k_2$ can be approximate by Kk_2,

$$k_q = \frac{k_2}{k_{-d} + k_2} k_d \qquad (14)$$

where K is the equilibrium constant for formation of the encounter complex. The observed decrease in k_q can therefore be due to either a change in K or k_2.

It should be noted at this point that k_d does not change drastically in the micellar, compared to the homogeneous, phase. From both ^{23}Na NMR[27] and VO^{2+} electron spin relaxation times,[4a] the mobility of counterions bound to alkyl sulfate micelles is known to be extremely high. The ions are able to diffuse along the micelle's surface at rates nearly equal to those found in homogeneous solution.

The above arguments suggest that the stabilization of the encounter complex is responsible for the slower quenching rate in micellar solution. Since the environment around a micelle is highly polar, ionic species will be stabilized relative to the H_2O/EtOH solution. In comparing the net stabilization of reactants and products in Scheme I, a decision concerning the stabilization of a M^{n+} ion relative to a $M^{(n-1)+}$ and pyrene^{+1} ion must be made. Since the pyrene radical cation is highly delocalized, it will not be stabilized by the increased polarity to the same extent as a small, localized ion. Consequently, the reactants will be stabilized to a greater extent than the products. This results in the generally smaller value of k_q.

Also shown in Table III are relative values for $k_q^{H_2O}$. Clearly, there is a relationship between the value of $k_q^{H_2O}$ and the micelle's effect on the quenching process. As the homogeneous quenching becomes more efficient, the effect of micellarization increases. This can be understood with the aid of the Hammond Postulate. In the very efficient extreme, the encounter complex should more resemble products. The increased polarity of the micellar environment will then result in substantial stabilization of the reactants and very little of the complex. This will drastically reduce K and result in a lower value of k_q. On the other hand, the encounter complex should resemble starting material in the inefficient extreme. The starting material and complex will be stabilized by more nearly equal amounts and the change in K will be reduced. This results in a smaller effect on k_q due to micellarization.

Table III. Ratio of Rate Constants for Pyrene Fluorescence Quenching in Homogeneous and Micellar Phases, Ionic and Hydrated Radii of the Metal Ion Quenchers, and Relative Rates of Quenching in Homogeneous Solution

metal ion	$k_q^{H_2O}/k_q^m$	radius, Å: ionic[a]	radius, Å: hydrated[b]	k_q^{rel} [c]
Cu^{2+}	189[d]	0.92	4.19	1.00
Tl^{+}	229	1.51	3.30	0.62
Cr^{3+}	136	0.55	4.61	0.36
Eu^{3+}	39	0.95	4.50[e]	0.13
Co^{2+}	100	0.70	5.23	0.07
Mn^{2+}	76	0.80	4.38	0.04

[a] From Reference 16. [b] From Reference 17. [c] Relative quenching rate constant in homogeneous solution. [d] Reference 9. [e] Estimated based on data for other lanthanides.

Summary

The binding of a metal ion to an anionic micelle is not always dictated by the apparent charge of the metal ion. The cases where the Bjerrum theory does not seem to apply can usually be explained by considering the known aqueous chemistry of the specific ions.

Upon micellarization, the quenching rate constants uniformly decrease for all metal ions. The magnitude of this decrease is dependent upon the efficiency of the quenching. The more efficient the quenching, the greater the effect of micellarization. This can

Scheme I

$$M^{+n} + P^* \underset{k_{-d}}{\overset{k_d}{\rightleftharpoons}} M^{n+}\cdots P^* \xrightarrow{k_2} M^{(n-1)+} + P^+$$

(21) Laswick, J. A.; Plane, R. A. *J. Am. Chem. Soc.* **1959**, *81*, 3565.
(22) Smith, R. A.; Martell, A. E. "Critical Stability Constants"; Plenum Press: New York, 1976; Vol. 4.
(23) For a review of micelle structure see: Menger, F. M. *Acc. Chem. Res.* **1979**, *12*, 111.
(24) Rodgers, M. A. J.; DaSilva, M. F.; Wheeler, E. *Chem. Phys. Lett.* **1978**, *53*, 165.
(25) Mukerjee, P.; Cardinal, J. R. *J. Phys. Chem.* **1978**, *82*, 1620.
(26) Weller, A. *Prog. React. Kinetics* **1961**, *1*, 187.
(27) Stibs, P.; Lindman, B. *J. Colloid Interface. Sci.* **1974**, *46*, 177.

be explained by assuming an encounter complex is involved in the quenching act. The micelle's environment is very polar and results in a decrease in the equilibrium constant for formation of this complex.

Acknowledgment. This work was supported by grants from the donors of the Petroleum Research Fund, administered by the American Chemical Society, the Research Corporation and the National Science Foundation (No. ISP-8011453).

[1-^{2}H]Allyl Radical: Barrier to Rotation and Allyl Delocalization Energy

Hans-Gert Korth, Heinrich Trill, and Reiner Sustmann*

Contribution from the Institut für Organische Chemie, Universität Essen, D-4300 Essen 1, West Germany. *Received October 6, 1980*

Abstract: Syn and anti [1-^{2}H]allyl radicals are generated from deuterated allyl phosphites by attack of *tert*-butoxy radicals, and their interconversion is studied in the temperature range of 50–110 °C. Steady-state kinetic analysis together with time-resolved measurements of the diffusion-controlled recombination kinetics yield an allyl rotational barrier of 15.7 ± 1.0 kcal/mol (log A = 13.5 ± 0.5). From this a value of 14.0–14.5 kcal/mol is deduced for the allyl delocalization energy.

The stereomutation (**1** ⇌ **2**) of allyl radicals, observed for the first time by Walling and Thaler[1] and later detected several times,[2-6] is of importance with respect to synthetic work involving allyl radicals and it is also connected to the problem of allyl delocalization energy.

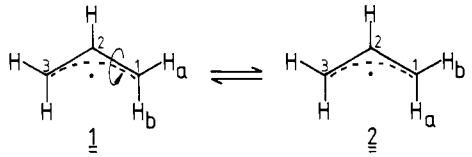

1 **2**

The qualitative observations provoked quantitative studies[7-12] to determine rotational barriers in these radicals. Table I records values which have been reported so far. Besides the first entry for 1-methylallyl radical, the values were obtained by electron spin resonance (ESR) methods, and in most cases E_a has been evaluated.

Attempts to determine the rotational barrier for the unsubstituted allyl radical by line-shape analysis of its ESR spectrum have failed so far. In experiments, the temperature region where line-shape effects might occur could not be reached.[13] From these studies a lower limit of 17 kcal/mol for the rotational barrier was deduced (for a discussion of this value, see below).

We now report an investigation for an "almost" unperturbed allyl radical that uses a kinetic procedure developed by Hamilton and Fischer for the neophyl rearrangement.[14] The method, also applied to the isomerization of *syn*-1-*tert*-butylallyl radical and the *syn-anti*-1-cyanoallyl radicals (Table I), requires the distinction of syn and anti 1-substituted allyl radicals. This was achieved by incorporating deuterium stereospecifically in the 1 position. Isomerization of **3** and **4** as a function of temperature enables the determination of the energy barrier. The close connection of this value with allyl delocalization energy will be discussed.

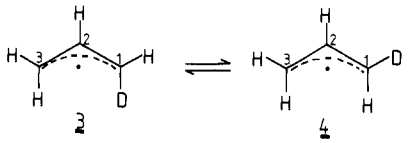

3 **4**

Radical Generation

Even though the allyl radical is stabilized, it belongs to the class of transient radicals. An ESR spectroscopic study, therefore, has to be carried out under conditions of continuous radical generation. Triallyl phosphite as radical precursor proved to be most suited for our analysis. Photolysis of di-*tert*-butyl peroxide in the presence of triallyl phosphite has been shown to yield **1** selectively in high concentration at temperatures >−90 °C.[15,16]

Selectively deuterated triallyl phosphites were obtained in 48–67% yield by the reaction of deuterated allyl alcohols with phosphorus trichloride.[17] Cis and trans deuterated allyl alcohols were prepared according to eq 1 and 2. Contrary to reports in

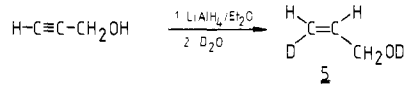

(1)

5

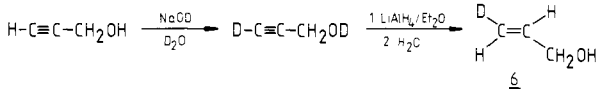

(2)

6

literature,[18,19] the reduction of sterically nonhindered propargylic alcohols does not proceed stereospecifically. ^{1}H NMR, ^{13}C NMR, IR, and high-resolution mass spectrometry indicated for **5** and **6** the presence of allyl alcohols which were deuterated in different positions. The isomer distribution, however, could not be determined accurately by these techniques. The ESR spectra of the

(1) C. Walling and W. A. Thaler, *J. Am. Chem. Soc.* **83**, 3877 (1961).
(2) W. A. Thaler, A. A. Oswald, and B. E. Hudson, *J. Am. Chem. Soc.* **87**, 3877 (1961).
(3) W. P. Neumann, H.-J. Albert, and W. Kaiser, *Tetrahedron Lett.*, 2041 (1967); W. P. Neumann and R. Sommer, *Liebigs Ann. Chem.* **701**, 28 (1967); H.-J. Albert, W. P. Neumann, W. Kaiser, and H.-P. Ritter, *Chem. Ber.* **103**, 1372 (1970).
(4) D. B. Denney, R. M. Hoyte, and P. T. McGregor, *J. Chem. Soc., Chem. Commun.*, 2041 (1967).
(5) R. M. Hoyte and D. B. Denney, *J. Org. Chem.*, **39**, 2607 (1974).
(6) I. B. Afanas'ev, I. V. Mamontova, I. M. Filipova, and G. I. Samokhvalov, *Zh. Org. Khim.* **7**, 866 (1971).
(7) R. J. Crawford, J. Hamelin, and B. Strehlke, *J. Am. Chem. Soc.*, **93**, 3810 (1971). This value may be in error, due to wall effects in the kinetic measurements (R. J. Crawford, private communication).
(8) P. J. Gorton and R. Walsh, *J. Chem. Soc., Chem. Commun.*, 783 (1972).
(9) R. Sustmann and H. Trill, *J. Am. Chem. Soc.* **96**, 4343 (1974).
(10) R. Sustmann, H. Trill, F. Vahrenholt, and D. Brandes, *Chem. Ber.*, **110**, 255 (1977); the difference to the activation parameters reported in ref 10 stems from the improved determination of the activation energy for recombination.
(11) R. Sustmann and D. Brandes, *Chem. Ber.* **109**, 354 (1976).
(12) B. E. Smart, P. J. Krusic, P. Meakin, and R. C. Bingham, *J. Am. Chem. Soc.* **96**, 7382 (1974).
(13) P. J. Krusic, P. Meakin, and B. E. Smart, *J. Am. Chem. Soc.* **96**, 6211 (1974).
(14) E. J. Hamilton Jr. and H. Fischer, *Helv. Chim. Acta* **76**, 795 (1973).
(15) P. J. Krusic and J. K. Kochi, *J. Am. Chem. Soc.* **91**, 3944 (1969).
(16) A. G. Davies, M. J. Parrott, and B. P. Roberts, *J. Chem. Soc., Perkin Trans. 2*, 1066, (1976).
(17) K. Sasse, *Methoden Org. Chem.* (Houben-Weyl) **12**(2), 55 (1973).
(18) J. Attenburrow, A. F. B. Cameron, J. H. Chapman, R. M. Evans, B. A. Hems, A. B. A. Jansen, and T. Walker, *J. Chem. Soc.*, 1094 (1952).
(19) R. A. Raphael, "Acetylenic Compounds in Organic Synthesis", Butterworth, London, 1955, p 29.

0002-7863/81/1503-4483$01.25/0